Effects of Modal Symmetry on Transonic Aeroelastic Characteristics of Wing-Body Configurations

Guru P. Guruswamy* and Eugene L. Tu†
NASA Ames Research Center, Moffett Field, California

To study accurately the transonic aeroelastic characteristics, it is important to model the full aircraft configuration, including asymmetry. Recently, an accurate method of computing unsteady transonic flows on full-span wing-body configurations was developed using the transonic potential flow theory. In this work, the method is further developed to account for the aeroelasticity of full-span wing-body configurations. This is accomplished by simultaneously integrating the unsteady aerodynamic forces and modal structural equations of the wing-body configurations. To validate the method, aeroelastic computations are made for a wing-body configuration with a rectangular wing. The aeroelastic responses of this configuration are correlated with the responses of a similar isolated wing. The comparisons are favorable. Aeroelastic computations associated with symmetric and antisymmetric modes are also made to study the influence of modal asymmetry on responses. This new development is further illustrated by computing the aeroelastic characteristics of a typical fighter aircraft. The results from this study will be useful in accurately computing the transonic flutter boundaries of aircraft, including those associated with asymmetric modes.

Introduction

ACCURATE computations of unsteady forces on full aircraft configurations are required to predict aeroelastic characteristics of aircraft, especially in the transonic regime where unsteady aerodynamics are characterized by moving shock waves over aerodynamic bodies, such as wings or fuselage. Aerodynamic forces are nonlinear and are very sensitive to changes in configurations caused by additional components and by changes in flow parameters. For example, recent studies[1] have shown that the addition of tip missile aerodynamics significantly influences the aeroelastic stability of wings, and in the transonic regime, rapid variations in the pressure distributions with increasing Mach number result in an unsafe aeroelastic phenomenon known as the "transonic dip."[2]

Asymmetry can be encountered for an aircraft either by configuration or by flow conditions. Configuration asymmetry can be caused by asymmetric static loads, such as on aircraft carrying stores, or it may be inherently present, as is the case for the oblique-wing aircraft. Effects of asymmetry on aeroelasticity can be more intense in the transonic regime, where the flow is nonlinear and contains moving shock waves. Experimental investigations[3] have shown that in some cases, the flutter speeds associated with antisymmetric modes are different than, and sometimes less than, those associated with the symmetric modes for the same wing. Therefore, to accurately compute the flutter speeds, it is important to model the full aircraft configuration, including asymmetry.

To accomplish the presented requirements for accurate aeroelastic analysis, a theoretical modeling of transonic flows requires the solution of time-dependent, nonlinear, partial differential equations that should be solved by a robust, time-accurate method. Recently, an accurate method of computing unsteady transonic flows on full-span wing-body configurations was developed using the transonic small-perturbation (TSP) theory.[4] This new capability was demonstrated by computing unsteady transonic flows over full-span wing-body configurations undergoing both symmetric and antisymmetric modal motions. Significant differences were found in the aerodynamic results between symmetric and antisymmetric modes. This new capability was incorporated into the code ATRAN3S, the NASA Ames version of the Air Force/NASA code XTRAN3S.[5] ATRAN3S, also known as XTRAN3S-Ames, is the most advanced code in use for both aerodynamic and aeroelastic analyses in the transonic regime. This code is currently being used for routine aeroelastic applications[6] of wings and to validate the development of unsteady codes based on the Euler/Navier-Stokes equations. The purpose of the present study is to further extend the capability of the ATRAN3S code to handle the aeroelasticity of full aircraft.

In this work, the technique[7] of simultaneously integrating the unsteady aerodynamic forces and modal structural equations is extended for full-span wing-body configurations. This is accomplished by accurately modeling both the aerodynamics[4] and the structural properties of the full-span wing-body configuration. To validate the method, aeroelastic computations were made for a wing-body configuration with a rectangular wing. The aeroelastic responses of this configuration are correlated with the responses of a similar isolated wing case. Aeroelastic computations associated with symmetric and antisymmetric modes are also made to study the influence of modal asymmetry on responses. This new development is further illustrated by computing the aeroelastic characteristics of a typical fighter aircraft configuration.

The present work is done in conjunction with the further development of ATRAN3S, which is being developed for general purpose computations of transonic unsteady aerodynamics and aeroelasticity of full aircraft. At present, this code is capable of computing flows over wings with tip missiles and

Presented as Paper 88-2308-CP at the AIAA/ASME/ASCE/AHS 29th Structures, Structural Dynamics and Materials Conference, Williamsburg, VA, April 18–20, 1988; received May 7, 1988; revision received Aug. 13, 1988. This paper is declared a work of the U.S. Government and therefore is in the public domain.

*Research Scientist; currently, Principal Analyst, Sterling Federal Systems Inc., Palo Alto, CA. Associate Fellow AIAA.

†Research Scientist. Member AIAA.

active control surfaces. With the development presented in this paper, the capability of the code will be close to computing flows on almost complete aircraft configurations. Since the present study models the full span of the wing, aeroelasticity associated with asymmetric modes of aircraft carrying stores and asymmetric configurations such as the oblique wing can be successfully simulated. Because of the use of the TSP equation, the computational time is practical for computationally intensive aeroelastic calculations.

Formulation of Unsteady Transonic Flow Equations

The coordinate system used in this analysis is shown in Fig. 1. The three-dimensional, unsteady, transonic small-perturbation equation of motion used in this analysis is given by[8]

$$A\phi_{tt} + B\phi_{xt} = [E\phi_x + F\phi_x^2 + G\phi_y^2]_x + [\phi_y + H\phi_x\phi_y]_y + [\phi_z]_z \tag{1}$$

where

$$A = M_\infty^2 \qquad B = 2M_\infty^2 \qquad E = (1 - M_\infty^2)$$

$$F = -\left(\frac{1}{2}\right)(\gamma + 1)M_\infty^2 \qquad G = -\left(\frac{1}{2}\right)(\gamma - 3)M_\infty^2$$

$$H = -(\gamma - 1)M_\infty^2$$

and ϕ is the disturbance velocity potential, M_∞ is the freestream Mach number, and γ is the ratio of specific heats. The flowfield boundary conditions used are

Far downstream:

$$\phi_x + k\phi_t = 0 \tag{2a}$$

Far upstream:

$$\phi = 0 \tag{2b}$$

Far above and below:

$$\phi_z = 0 \tag{2c}$$

Far spanwise:

$$\phi_y = 0 \tag{2d}$$

Trailing vortex wake:

$$[\phi_z] = 0 \tag{2e}$$

$$[\phi_x + k\phi_t] = 0 \tag{2f}$$

where [ ] denotes the jump in the quantity across the vortex sheet.

The thin wing-surface-flow tangency condition satisfied at the mean chord plane is given by

$$\phi_z = f_x + kf_t \tag{3}$$

where $f(x)$ denotes the airfoil surface function and $k = \omega c/U_\infty$ is the reduced frequency based on the full chord. Variable ω is the frequency in rad/s, c is a reference chord length, and U_∞ is the freestream velocity.

The preceding equations are transformed so that a swept, tapered wing can be analyzed by using a finite-difference mesh aligned with the leading and trailing edges of the wing. The transformed equation is solved by the time-accurate alternating-direction implicit finite-difference scheme. Details are given in Ref. 4.

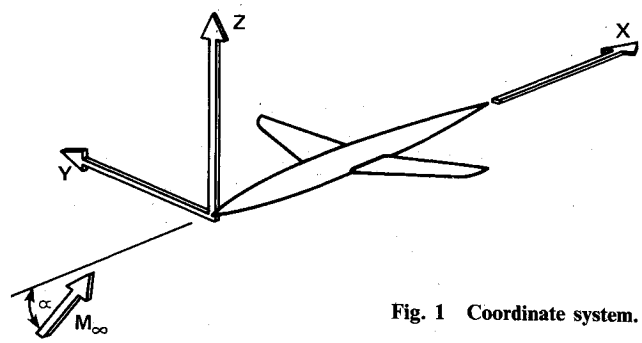

Fig. 1 Coordinate system.

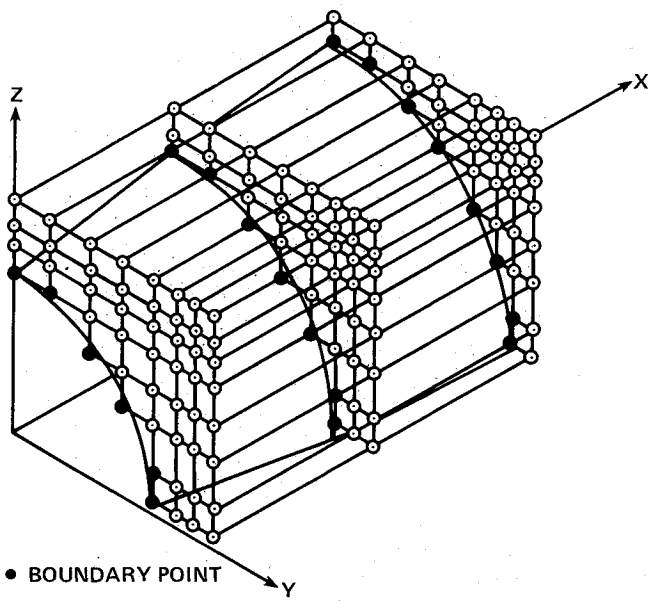

Fig. 2 Body boundary points.

Aerodynamic Modeling of Fuselage

The fuselage is modeled as a body based on the small-perturbation theory by following the procedure described in Sec. 1.3 of Ref. 9. For a body described by the equation $g(x,y,z,t) = 0$, the small-perturbation flow tangency boundary condition on the surface of the body becomes[9]

$$kg_t + (1 + \phi_x)g_x + \phi_y g_y + \phi_z g_z = 0 \tag{4a}$$

To the first order, this equation becomes

$$kg_t + g_x + \phi_y g_y + \phi_z g_z = 0 \tag{4b}$$

In the present method, the fuselage is treated in a rectangular mesh system as shown in Fig. 2. The mesh is constructed so that points lie reasonably close to the fuselage surface. Depending on the mesh fineness, the grid points may lie either inside or outside of the fuselage surface. The boundary condition [Eq. (4)] is treated implicitly to give accurate and fast solutions as follows.

The aerodynamic equation of motion [Eq. (1)] is solved by the alternating-direction implicit scheme using three sweeps. In the x sweep, the boundary condition [Eq. (4)] is imposed explicitly since it does not involve any derivatives of the potential in the x direction. In the y sweep, the ϕ_y term is implicitly treated and the ϕ_z term is explicitly treated. In the z sweep, the ϕ_z term is implicitly treated and the ϕ_y term is explicitly treated. The two-point extrapolated differences are substituted for ϕ_y and ϕ_z at the boundary points.

This approach requires an efficient grid-generation and body-boundary-point identification scheme. In this work, a numerical scheme that generates a grid for accurate modeling of a given wing-body configuration was developed and incorporated in ATRAN3S (XTRAN3S-Ames). This scheme gives a grid that is fine around the wing-body and stretches smoothly far enough in the flowfield to reduce the effect of far-field boundary reflections. It clusters grid lines along the leading and trailing edges of the wing and gives adequate grid lines on the wing and the body. Figure 3 shows the grid in the $x-y$ plane obtained by the present grid-generation scheme for the RAE wing-body configuration. The boundary grid points on the body (Fig. 2) are automatically identified by the scheme without any user interface. In order to impose the boundary condition [Eq. (4)], which is in the Cartesian coordinate system, the grid-generation scheme generates a Cartesian physical grid near the body, as shown in Fig. 3 for the RAE wing-body configuration. Thus, the metric term ξ_y is zero for all grid points on the body.

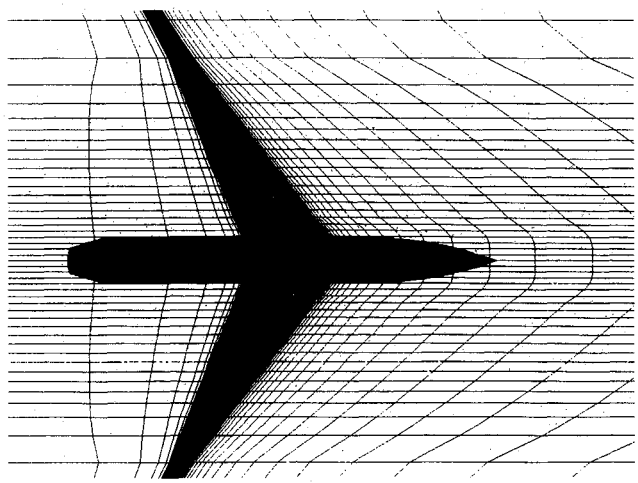

Fig. 3 Grid in x-y plane for the RAE wing-body configuration.

Aeroelastic Equations of Motion

The governing aeroelastic equations of motion of a flexible wing are obtained by using the Rayleigh-Ritz method (Ref. 10, Chap. 3). In this method the resulting aeroelastic displacements at any time are expressed as a function of a finite set of selected modes. The contribution of each selected mode to the total motion is derived by Lagrange's equation. Furthermore, it is assumed that the deformation of the continuous-wing structure can be represented by deflections at a set of discrete points. This assumption facilitates the use of discrete structural data, such as the modal vector, the modal stiffness matrix, and the modal mass matrix. In this study, the finite-element method is employed to obtain the modal data. The stiffness and mass of both the right and left wings are included in the analysis, and it is assumed that the body is rigid.

It is assumed that the deformed shape of the wing can be represented by a set of discrete displacements at selected nodes. From the modal analysis, the displacement vector $\{d\}$ can be expressed as

$$\{d\} = [\psi]\{q\} \tag{5}$$

where $[\psi]$ is the modal matrix and $\{q\}$ is the generalized displacement vector. The final matrix form of the aeroelastic equations of motion is

$$[M]\{\ddot{q}\} + [G]\{\dot{q}\} + [K]\{q\} = \{F\} \tag{6}$$

where $[M]$, $[G]$, and $[K]$ are modal mass, damping, and stiffness matrices, respectively. The aerodynamic force vector $\{F\}$ is defined as $(\frac{1}{2})\rho U_\infty^2[\psi]^T[A]\{\Delta C_p\}$, where ρ is the freestream density, U_∞ is the freestream velocity, ΔC_p is the pressure jump at the aerodynamic control points, and $[A]$ is the diagonal area matrix of the aerodynamic control points.

These equations of motion are solved by numerical integrating Eq. (6) in time by the linear acceleration method.[7] The step-by-step integration procedure for obtaining the aeroelastic response is performed as follows. Assuming that freestream conditions and wing surface boundary conditions were obtained from a set of selected starting values of the generalized displacement, velocity, and acceleration vectors, the generalized aerodynamic force vector $\mathbf{F(t)}$ at time $t + \Delta t$ was computed by solving Eq. (1). Using this aerodynamic vector, the generalized displacement, velocity, and acceleration vectors for the time level $t + \Delta t$ are calculated by numerically integrating Eq. (6). From the generalized coordinates computed at the time level $t + \Delta t$, the new boundary conditions on the surface of the wing are computed. With these new boundary conditions, $F(t)$ at the next time level is computed by using Eq. (1). This process is repeated every time-step to solve the aerodynamic and structural equations of motion forward in time until the required response is obtained.

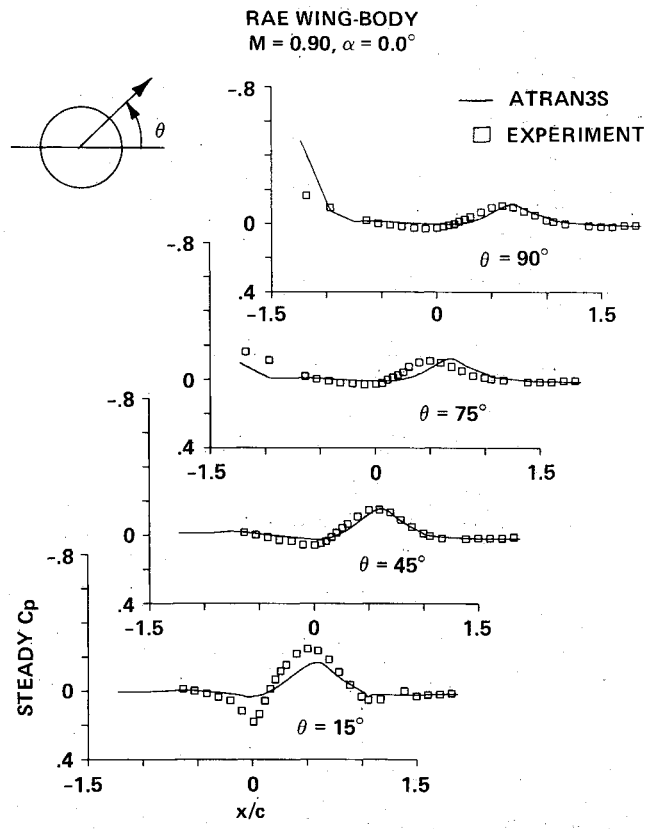

Fig. 4 Steady pressure distributions on the body of the RAE wing-body configuration.

Results

Validation of Aerodynamic Modeling

Accurate computations of unsteady transonic loads are essential to obtain accurate aeroelastic responses of the full aircraft. Steady and unsteady aerodynamic results from the present modeling compare well with other theories and experiments. These results are shown in detail in Ref. 4. Figure 4 illustrates the good comparison between computed and measured steady aerodynamic pressures on the fuselage of the RAE wing-body configuration. Results of unsteady calculations of a rectangular wing-cylinder configuration compare reasonably well with both the theoretical and experimental data for a wall-mounted wing-alone configuration, as shown in Fig. 5.

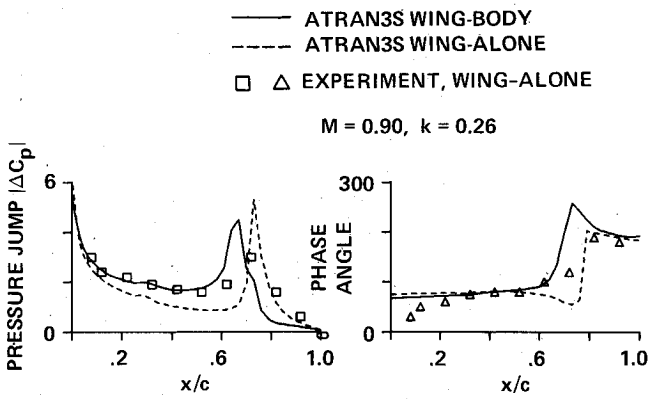

Fig. 5 Comparison of unsteady pressures in computation (wing-cylinder and wing-alone) and experiment (wing-alone).

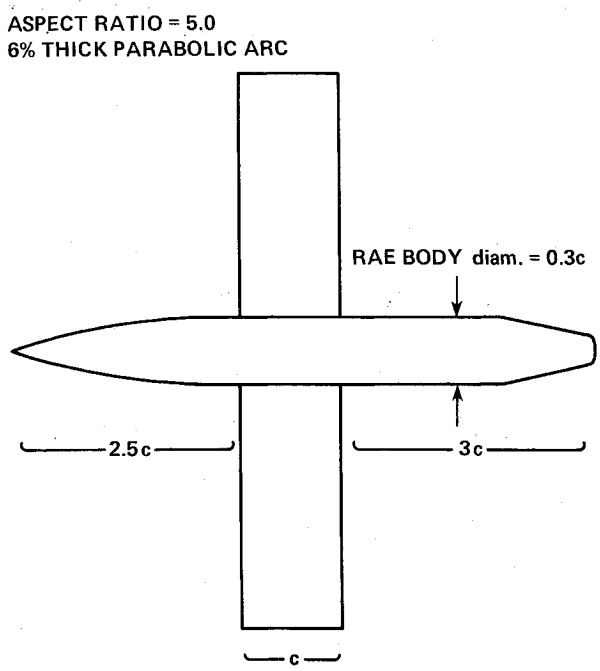

Fig. 6 The rectangular RAE wing-body configuration.

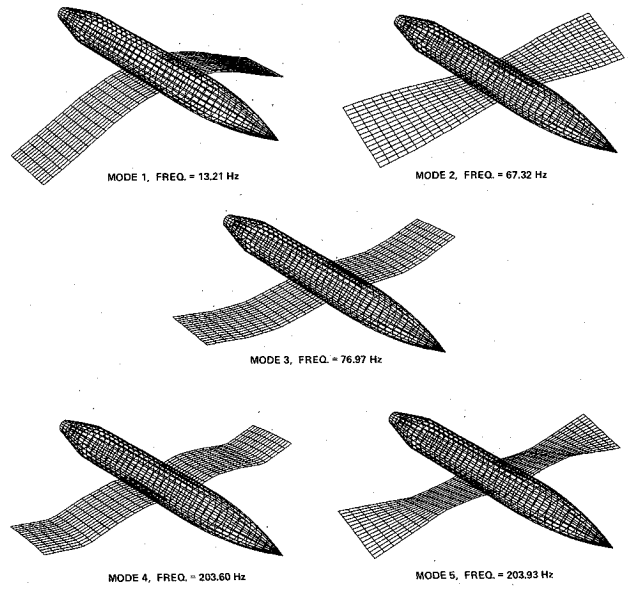

Fig. 7 Symmetric mode shapes of the rectangular wing-body configuration.

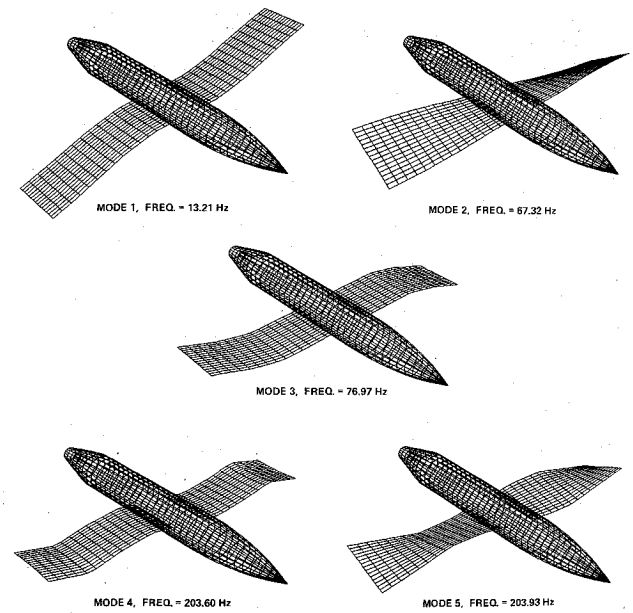

Fig. 8 Antisymmetric mode shapes of the rectangular wing-body configuration.

Unsteady Computations

Aeroelastic response analyses are conducted for a uniform rectangular wing-body configuration shown in Fig. 6. The rectangular wing used in these analyses has an aspect ratio of 5.0 and a parabolic-arc airfoil section with a 6% thickness. The body used in this configuration is the same as the body for the RAE wing-body configuration.[4] The mode shapes and frequencies required for the modal equations of motion Eq. (5) were obtained from a 16-degree-of-freedom rectangular finite element.[11] In computing the mode shapes, it is assumed that the body is rigid. The symmetric and antisymmetric mode shapes and frequencies of the rectangular wingbody configuration are shown in Figs. 7 and 8, respectively. These modes were constructed using the five fundamental modes of a rectangular wing that has the same structural properties of either the right or left wing of the wing-body configuration.

In order to understand the differences in aerodynamics between the symmetric and antisymmetric mode shapes, a detailed unsteady aerodynamic analysis is performed on the rectangular wing-body configuration. Previous studies[12] have shown that for this particular rectangular wing, the twisting mode plays a predominant role in determining the flutter characteristics of the wing. Therefore, for this analysis, the magnitude and phase of the lift and moment are computed for the first symmetric and antisymmetric twisting modes. Computations were made at three Mach numbers (0.795, 0.875, and 0.905). For all Mach numbers, a reduced frequency of 0.20 was selected based upon the measured flutter frequencies given in Ref. 13.

The unsteady sectional lift and moment results for three Mach numbers (0.795, 0.875, and 0.905) are shown for the full span of the wing in Figs. 9 and 10, respectively. The results in Figs. 9 and 10 show slight asymmetries near the body, though pure symmetric and antisymmetric modes were used in the analyses. It is noted that a moderately fine grid of size $82 \times 50 \times 40$ was used in the present computations. A finer grid is required to remove discrepancies near the body.

From Figs. 9 and 10, it is noted that small changes occur between the symmetric and antisymmetric modes when the

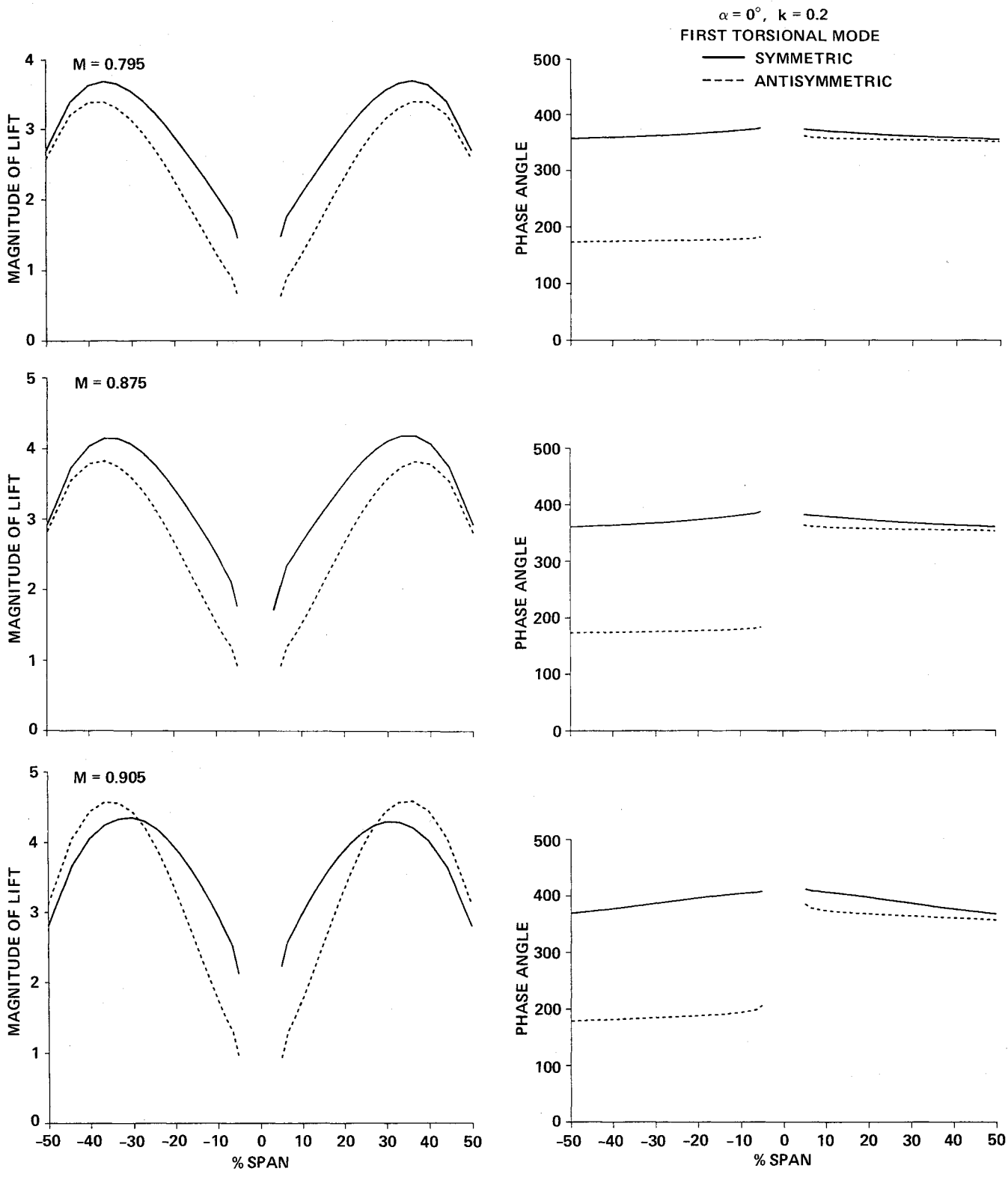

Fig. 9 Comparison of unsteady lift coefficients between symmetric and antisymmetric twisting modes for the rectangular wing-body configuration at three Mach numbers.

Mach number is increased from $M = 0.795$ to 0.875. Further results of unsteady analyses conducted at the additional Mach numbers of 0.836 and 0.851 indicate that the relative changes in the lifts and moments are small throughout the subsonic to transonic Mach number range of 0.795–0.875. However, dramatic differences between the symmetric and antisymmetric unsteady lifts and moments occur when the Mach number is increased from 0.875 to 0.905. At $M = 0.875$, magnitudes of lifts and moments are higher for the symmetric cases than for the antisymmetric cases for almost 100% of the wing span. However, at $M = 0.905$, the magnitudes of lift and moment for the symmetric cases are higher for only approximately 50 and 20% of the span, respectively. These trends have an important influence on the aeroelastic responses, which will be illustrated in the following section.

Aeroelastic Computations of the Rectangular Wing-Body

Using the modal data shown in Figs. 7 and 8, aeroelastic responses associated with symmetric and antisymmetric modes were computed at various Mach numbers and dynamic

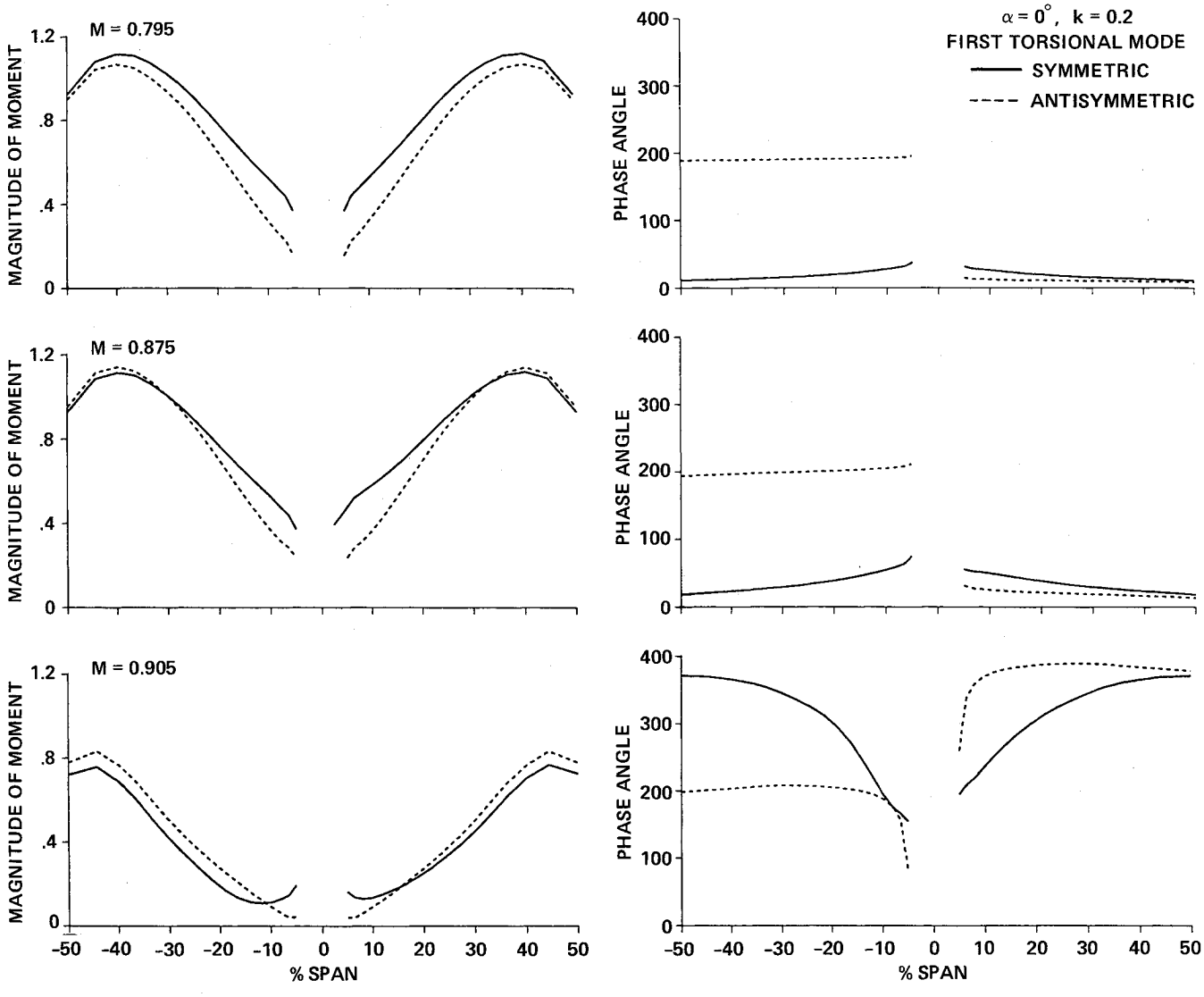

Fig. 10 Comparison of unsteady moment coefficients between symmetric and antisymmetric twisting modes for the rectangular wing-body configuration at three Mach numbers.

pressures. All responses were started with modally displaced initial conditions obtained by giving unit values to the first two generalized coordinates. All computations were made at dynamic pressures close to the fluttering speed. Results from aeroelastic analyses presented in this paper compare well with other computed[1] and experimental[13] aeroelastic results for wing-alone configurations. The flutter speeds associated with wing-body symmetric modes computed in this work and experimental results for a wing-alone configuration given in Ref. 13 differ by less than 10%. The modal data required for computations were computed accurately using the structural properties of the model. For example, the computed frequency of the first bending mode is about 7.5% less than the measured frequency. The favorable comparisons between computed and measured steady, unsteady, and aeroelastic results verifies the correct modeling of the fuselage.

Figures 11–13 illustrate the aeroelastic responses of the first three normal modes associated with both symmetric and antisymmetric modes at Mach numbers of 0.795, 0.875, and 0.905, respectively. As shown in Fig. 11, at $M = 0.795$ and a dynamic pressure of 1.28 psi, aeroelastic responses associated with the antisymmetric modes have significantly less damping than the corresponding response associated with the symmetric modes. For this particular configuration and flow condition, results shown in Fig. 11 indicate that the flutter speed is lower for the antisymmetric case than for the symmetric case. Other experimental studies[3] have shown that in some cases the flutter speeds associated with antisymmetric modes are less than those associated with the symmetric modes for the same wing. A detailed flutter analysis similar to the one performed in Ref. 12 shows that for this case, the antisymmetric flutter speed is lower than the symmetric flutter speed by 4.8%. Both the present theoretical results and the experimental results[3] emphasize the need to model full aircraft configurations, including asymmetry, to accurately compute flutter speeds.

Figure 12 shows response results at $M = 0.875$ and a dynamic pressure of 1.40 psi. From Fig. 12, it can be seen that the difference in the amount of damping between the symmetric and antisymmetric modal responses is significantly reduced when compared to those shown in Fig. 11 for $M = 0.795$. The flutter speeds associated with the symmetric and antisymmetric modes for this condition are almost equal. A detailed flutter analysis shows that for this case, the antisymmetric flutter speed is lower than the symmetric flutter speed by less than 2.0%.

Figure 13 shows response results at the high transonic Mach number of 0.905 and a dynamic pressure of 1.1 psi. In this case, there is a noticeable switch between the symmetric and antisymmetric modal response when compared to the previous two Mach numbers. The antisymmetric case has significantly more damping in both the first and second modal responses than does the symmetric case. For this case, it

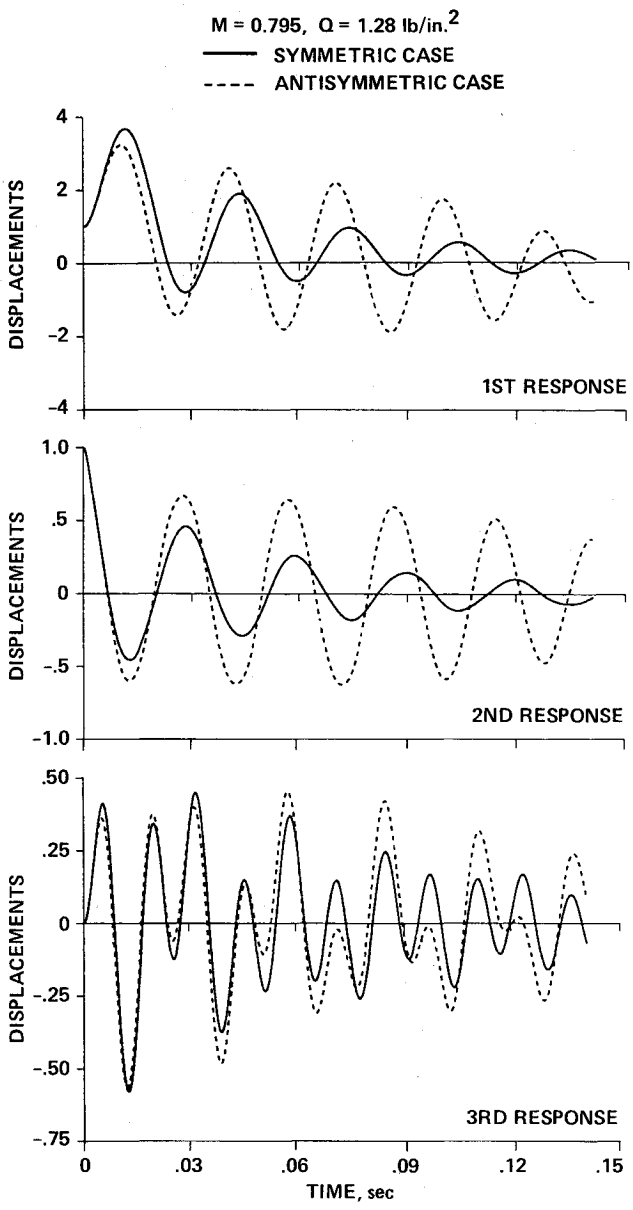

Fig. 11 Aeroelastic responses associated with symmetric and antisymmetric modes of the rectangular wing-body configuration at $M = 0.795$.

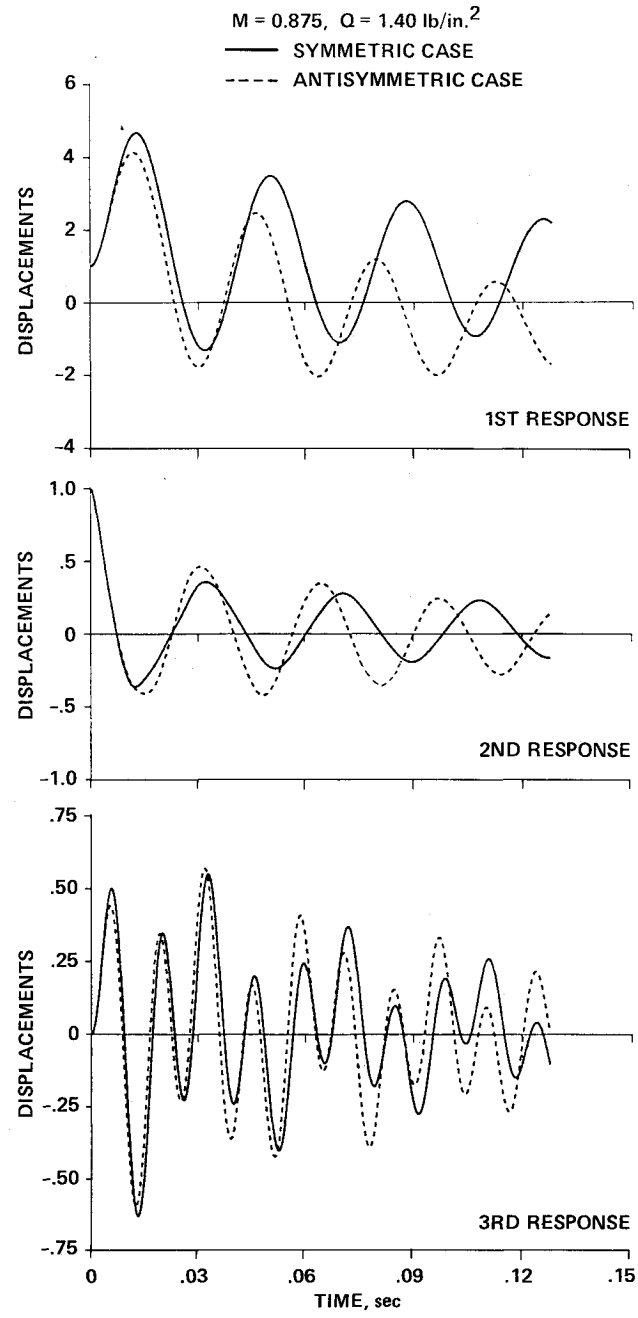

Fig. 12 Aeroelastic responses associated with symmetric and antisymmetric modes of the rectangular wing-body configuration at $M = 0.875$.

appears that the antisymmetric modes give a flutter-free condition, whereas the results for the corresponding symmetric modes are close to fluttering.

The comparisons between the aeroelastic responses associated with the symmetric and antisymmetric modes are summarized in Fig. 14. Figure 14 shows the second modal response (predominantly twisting mode) for five Mach numbers ranging from 0.795 to 0.905. For all Mach numbers, computations are made at dynamic pressures close to the fluttering speed of either the symmetric or antisymmetric modes. At $M = 0.795$, the antisymmetric case has less damping than the corresponding symmetric case. As the Mach number is increased, the difference in the amount of damping between the symmetric and antisymmetric cases decreases until a switch takes place at $M = 0.905$. This switch is a direct result of the sensitivity of transonic unsteady pressures to mode shapes. For example, significant changes took place in unsteady lifts and moments between $M = 0.875$ and 0.905 when the mode shape was changed from symmetric to antisymmetric.

In the present analyses, aeroelastic stabilities were studied by directly using the responses of the coupled modal displacements. Further conclusions can be made by postprocessing the responses to determine the damping using the other methods such as the logarithmic decrement technique. Results in this section illustrate the strong sensitivity of unsteady transonic forces and corresponding aeroelastic responses to mode shape symmetry.

Aeroelastic Computations of Typical Fighter Wing-Body

The development in this paper is demonstrated for a typical fighter configuration. The planform of the fighter aircraft configuration selected is given in Fig. 15. The wings of the fighter are based on aerodynamic and aeroelastic data available for the YF-17 aircraft.[14] Similar to the rectangular

wing-body configuration, the symmetric and antisymmetric mode shapes and frequencies are generated based on the wing mode shapes and frequencies given in Fig. 16. By using the modal data, aeroelastic response analysis was conducted at the transonic Mach number of 0.90 and an altitude of 30,000 ft. Symmetric and antisymmetric aeroelastic response results are shown in Fig. 17. For this configuration and flow condition, it is observed that the symmetric response has less damping than the antisymmetric response, indicating a lower flutter speed for the symmetric modes.

Conclusions

A procedure has been developed to conduct transonic aeroelastic analyses of full-span wing-body configurations. Both aerodynamic and structural properties of the full configuration are accurately modeled. Keeping the practical aeroelastic applications in view, the flow is modeled by using the transonic small-perturbation theory. Computed aerody-

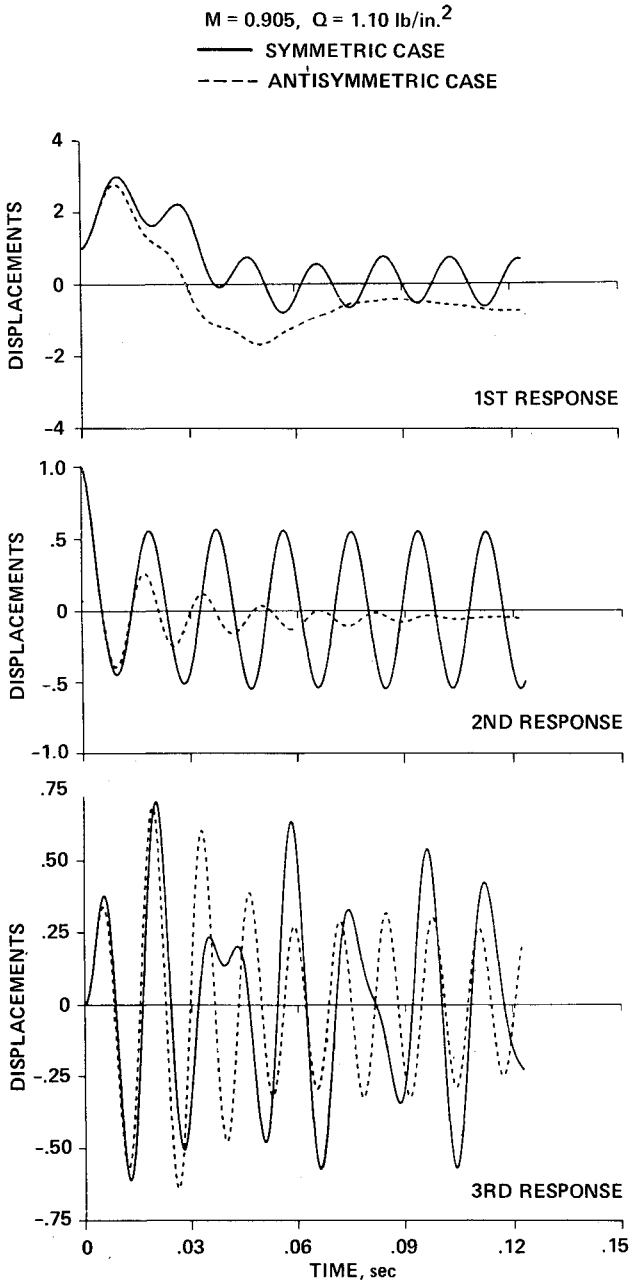

Fig. 13 Aeroelastic responses associated with symmetric and antisymmetric modes of the rectangular wing-body configuration at $M = 0.905$.

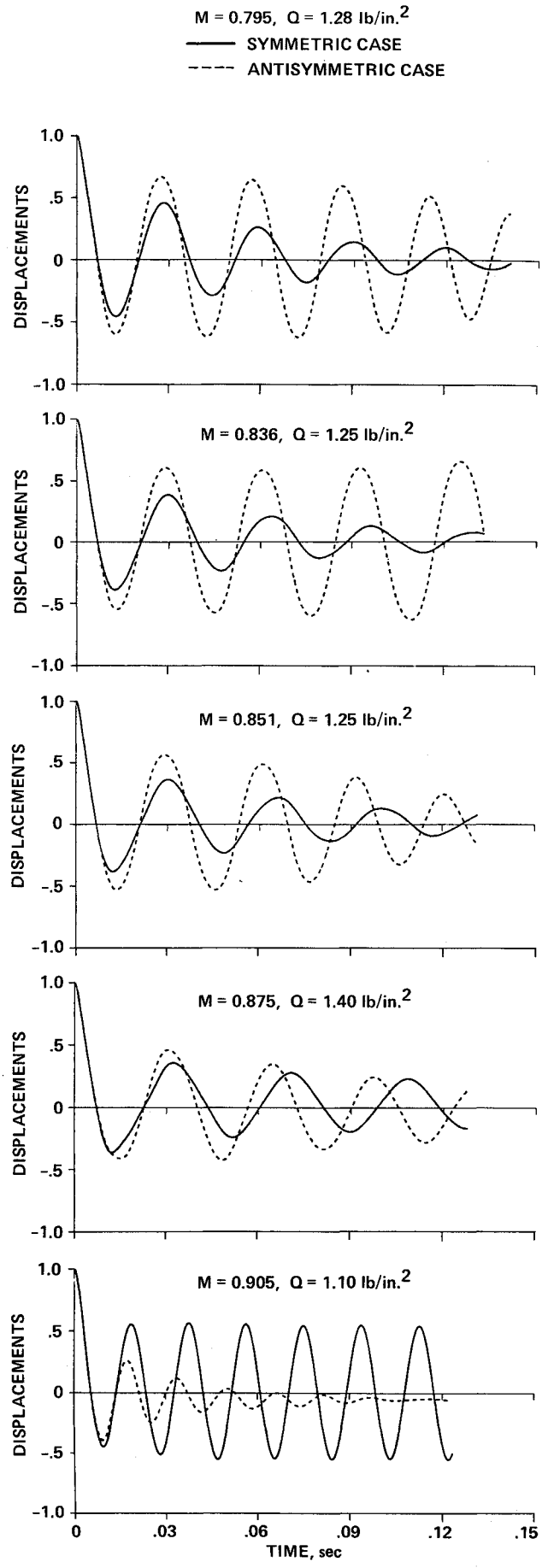

Fig. 14 Summary of aeroelastic responses of the second mode for five Mach numbers.

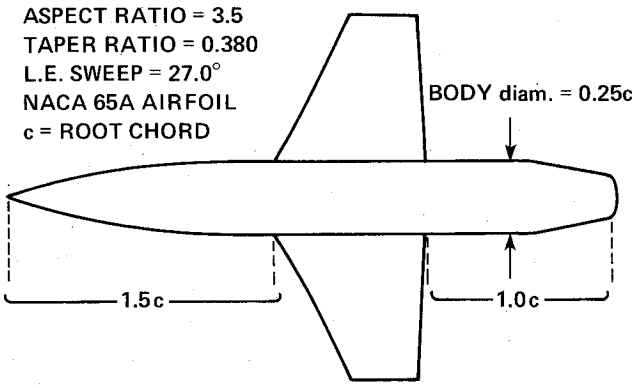

Fig. 15 Typical fighter wing-body configuration.

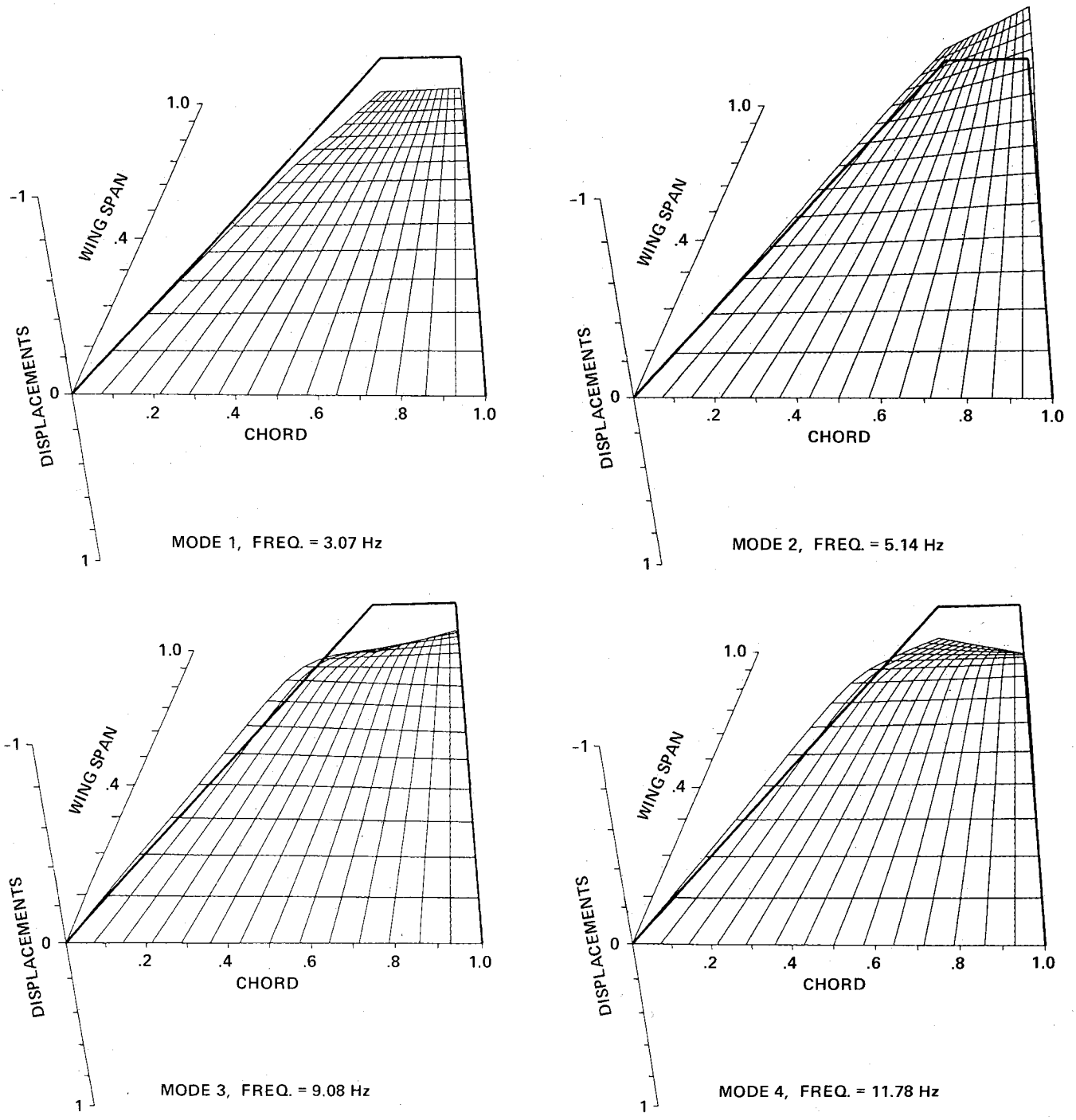

Fig. 16 Mode shapes of the fighter wing.

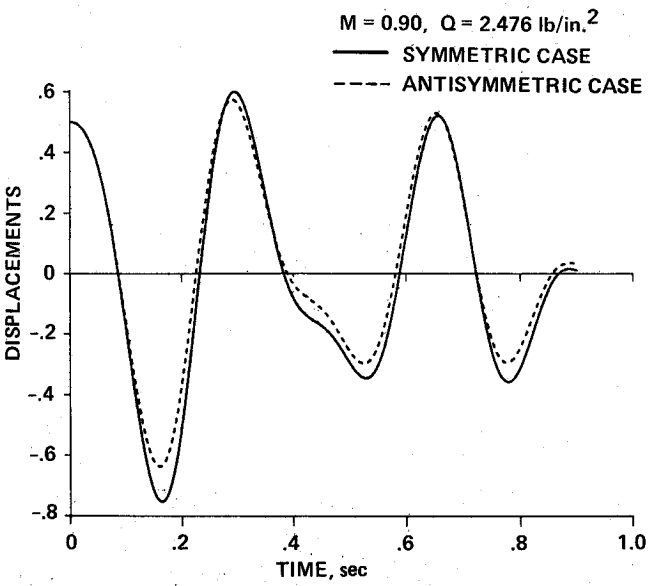

Fig. 17 Aeroelastic responses of first mode associated with symmetric and antisymmetric modes of the fighter wing-body configuration at $M = 0.90$.

namic and aeroelastic results compare well with the experimental results. Computations for a rectangular wing-body configuration show that the present procedure of coupling the aerodynamics and structures of full aircraft works successfully. Results show that, in some cases, the flutter speed associated with antisymmetric modes is less than that associated with symmetric modes. Furthermore, a correlation between the unsteady loads and the aeroelastic response of a wing is demonstrated. Results are also illustrated for a typical fighter wing-body configuration to demonstrate the practical application of this development in accurate flutter analysis of future advanced fighter aircraft. In this study, the full span of the wing is modeled by treating the left and right wings independently. As a result, aeroelasticity associated with asymmetric modes of aircraft can be successfully simulated. Since the present study is in the time domain, it can complement the wind-tunnel and flight tests as a "numerical flight simulator" and reduce the design cost considerably.

References

[1]Guruswamy, G. P., Goorjian, P. M., and Tu, E. L., "Transonic Aeroelasticity of Wings with Tip Store," *Journal of Aircraft*, Vol. 24, Oct. 1987, pp. 688–695.

[2]Ashley, H., "Role of Shocks in the 'Sub-Transonic' Flutter Phenomenon," *Journal of Aircraft*, Vol. 17, March 1980, pp. 187–197.

[3]Peloubet, R. P. and Haller, R. L., "Wind Tunnel Demonstration of an Active Flutter Supression System Using F-16 Model With Stores," Air Force Wright Aeronautical Labs, TR-83-3046, April 1983.

[4]Guruswamy, G. P. and Goorjian, P. M., "Unsteady Transonic Flow Simulation on a Full-Span Wing-Body Configuration," AIAA Paper 87-1240, June 1987.

[5]Huttsell, L. J. and Cooley, D. E., "The Background and Status of the Joint Air Force/NASA Transonic Unsteady Aerodynamic Program (XTRAN3S)," Air Force Wright Aeronautical Labs, TM-86-154-FIBRC, Jan. 1986.

[6]Guruswamy, G. P., Goorjian, P. M., Ide, H., and Miller, G. D., "Transonic Aeroelastic Analysis of the B-1 Wing," *Journal of Aircraft*, Vol. 23, July 1986, pp. 547–553.

[7]Guruswamy, P. and Yang, T. Y., "Aeroelastic Time Response Analysis of Thin Airfoils by Transonic Code LTRAN2," *Computers and Fluids*, Vol. 9, Dec. 1980, pp. 409–425.

[8]Yoshihara, H., "Formulation of the Three-Dimensional Transonic Unsteady Aerodynamic Problem," Air Force Flight Dynamics Lab, TR-79-3030, Feb. 1979.

[9]Landahl, M. T., *Unsteady Transsonic Flow*, Pergamon, New York, 1961, Chap. 1, Sec. 3.

[10]Bisplinghoff, R. L., Ashley, H., and Halfman, R. L., *Aeroelasticity*, Addison-Wesley, Reading, MA, 1957, Chap. 3.

[11]Guruswamy, G. P. and Yang, T. Y., "Special-Purpose Finite Element Programs," edited by T. Y. Yang, *Finite Element Structural Analysis*, Chap. 13, Prentice-Hall, Englewood Cliffs, NJ, 1986.

[12]Guruswamy, G. P., Tu, E. L., and Goorjian, P. M., "Transonic Aeroelasticity of Wings With Active Control Surfaces," *Proceedings of the 28th Structural Dynamics Conference*, AIAA, New York, 1987.

[13]Doggett, R., Rainey, A., and Morgan, H., "An Experimental Investigation of Aerodynamic Effects of Airfoil Thickness on Transonic Flutter Characteristics," NASA TM-X-79, 1959.

[14]Hwang, C., Winther, B. A., and Mills, G. R., "Demonstration of Active Wing/Store Flutter Supression Systems," Air Force Flight Dynamics Lab, TR-78-65, April 1978.